Journal of Thermal Analysis, Vol. 52 (1998) 615-630

TG/DTA, XRD AND NH_3-TPD CHARACTERIZATION OF LAYERED $VOPO_4 \cdot 2H_2O$ AND ITS Fe^{3+}-SUBSTITUTED COMPOUND

G. Bagnasco[1], *L. Beneš*[2], *P. Galli*[3], *M. A. Massucci*[3], *P. Patrono*[4], *M. Turco*[1] *and V. Zima*[2]

[1]Dipartimento di Ingegneria Chimica, Università 'Federico II', P. le Tecchio 80 80125-Naples, Italy
[2]Joint Laboratory of Solid State Chemistry, Academy of Sciences of Czech Republic and University of Pardubice, Studenska 84, 530 09 Pardubice, Czech Republic
[3]Dipartimento di Chimica, Università 'La sapienza', P. le Aldo Moro, 5-00185-Rome, Italy
[4]IMAI-CNR, Area della Ricerca, Via Salaria Km 29.6-00016-Monterotondo Scalo, Rome Italy

(Received September 25, 1997)

Abstract

Iron(III)-substituted vanadyl phosphate, $[Fe(H_2O)]_{0.20}VO_{0.80}PO_4 \cdot 2.25H_2O$ (FeVOP), has been prepared and characterized by XRD and TG/DTA analyses. The new compound is isomorphous with layered tetragonal $VOPO_4 \cdot 2H_2O$ (VOP), but it possesses a lower interlayer distance. Information on the reactivity and surface acidity of both VOP and FeVOP has been obtained by NH_3-TPD experiments. The hydrated materials adsorb high amounts of NH_3 (up to 2 mmol g^{-1}). Different ammonia-containing phases are formed, characterized by lower interlayer distances in comparison with the NH_3-free parent compounds. NH_3 is intercalated between the layers without displacement of water. The materials dehydrated by heat treatment at 450°C retain the layered structure but adsorb NH_3 only on the external surface. A wide variety of acid sites, from weak to strong, was observed. A mechanism is proposed for the NH_3- acid sites interaction. SEM micrographs of VOP and FeVOP are shown.

Keywords: Fe^{3+}-vanadyl phosphate, NH_3-TPD, surface acidity, TG/DTA, vanadyl phosphate, XRD

Introduction

Vanadium-phosphorus oxides (VPO) are employed as catalysts in several oxidation reactions of hydrocarbons [1–7]. The preparation of such materials generally occurs through an appropriate thermal treatment of vanadyl phosphate phases such as $VOPO_4 \cdot 2H_2O$ or $VOHPO_4 \cdot 0.5H_2O$. Although V^{4+} pyrophosphate, $(VO)_2P_2O_7$, is considered to be the active component in the partial oxidation of hydrocarbons such as that of *n*-butane to maleic anhydride, there is good evi-

1418–2874/98/ $ 5.00
© 1998 Akadémiai Kiadó, Budapest
Akadémiai Kiadó, Budapest
Kluwer Academic Publishers, Dordrecht

dence that the presence of other phases containing V^{5+}, like different $VOPO_4$ phases, is essential for the catalytic activity [2]. Under this aspect the new materials obtained by isomorphous substitution of VO groups of $VOPO_4 \cdot 2H_2O$ with trivalent metals such as Al, Ga, Fe, Cr, Mn [8, 9] that we have in part investigated for their thermal properties and structural modifications with temperature [10] could also have interesting catalytic properties, since it has been reported that the addition of different metals can improve the catalytic activity of VPO systems in oxidation reactions [11, 12].

The catalytic activity of VPO systems is likely to be influenced by the acidic properties due to the presence of VO groups [8, 13] acting as Lewis acid sites. The presence of these sites becomes evident by considering the structure of vanadyl phosphate. $VOPO_4 \cdot 2H_2O$ has a layered tetragonal structure formed by PO_4 tetrahedra linked to the VO groups [14, 15], arranged in such a fashion as to create 'pockets' in the interlayer region. Each vanadium atom, being pentacoordinated with oxygen atoms, is able to bind a basic molecule, so completing a (distorted) octahedral coordination. In the hydrated phase the complete coordination occurs through a $V...OH_2$ bond, while in the anhydrous phases this is obtained by the formation of a loose V...O bond between atoms of adjacent layers. This reasoning can also be made for the above mentioned M^{3+}-vanadyl phosphate compounds, isomorphous with $VOPO_4 \cdot 2H_2O$ and it is presumable that the metal substitutions will bring about interesting changes in the acidic properties of the different solids.

Works are reported in the literature dealing with intercalation of basic substances, such as amines or alcohols, into $VOPO_4$ phases [13, 16–19], with consequent increase in the interlayer distance of the host. Little research, however, has been devoted to the interaction with the simple base NH_3, although this substance is widely employed for the characterization of the acidic properties of solids. Ammonia intercalation can occur into anhydrous α_I-$VOPO_4$ [20], but the nature of this interaction has not been defined.

This paper reports on the thermal and structural characterization of the recently prepared iron-vanadyl phosphate with formula $[Fe(H_2O)]_{0.20}VO_{0.80}PO_4 \cdot 2.25H_2O$ and the results are compared with those obtained for pure vanadyl phosphate dihydrate [10]. The acidic properties of both $VOPO_4 \cdot 2H_2O$ and the Fe^{3+}-substituted compound, were studied by NH_3 thermal programmed desorption (TPD) technique, which is a suitable tool for the characterization of layered catalysts [21–23]. The solids treated with NH_3 were also characterized by XRD analyses and TG/DTA measurements.

Experimental

Preparation of materials

$VOPO_4 \cdot 2H_2O$ was prepared according to Ladwig [24], by refluxing 10 g of V_2O_5 (Fluka puriss. grade) in 300 ml of a 3.3 mol dm^{-1} H_3PO_4 (Carlo Erba RPE, highest purity product) solution. The compound $[Fe(H_2O)]_{0.20}VO_{0.80}PO_4\cdot 2.25H_2O$ was prepared similarly according to Melanova *et al.* [8], by adding to the vanadium pentoxide-phosphoric acid mixture an amount of $Fe(NO_3)_3\cdot 9H_2O$ (Carlo Erba RPE) such that the V/Fe molar ratio was 10/3. After 16 h reflux time, both suspensions were hot filtered, the yellow-green solids washed with cold distilled water and dried in air. Chemical analyses of the compounds were carried out as described in [9].

Materials characterization

A Philips PW 1100 model was used for taking the X-ray diffractograms (XRD) in air at room temperature (*r.t.*). A Freiberg Präzisionsmechanik model HZG-4 was employed for the X-ray measurements performed in the temperature range 20–250°C. In this case, the powder samples were placed on a corundum plate (with thermocouple) and heated to the desired temperature. For both diffractometers Ni-filtered CuK_α radiation was used; the 2θ measurements were accurate to 0.05° (2θ angles range examined: 5–45°); silicon (a=5.43055 Å) was employed as an external standard.

Thermal analyses were performed with a Stanton Redcroft STA 801 model simultaneous TG/DTA thermoanalyzer (ignition up to 1000°C, heating rate 10°C min^{-1}, in an air flow). The water content of the solids was determined from the TG measurements.

BET surface areas were measured by N_2 adsorption at –196°C on a Quantachrom CHEMBET 300 instrument.

NH_3 TPD measurements were carried out in a flow apparatus with a TCD detector. The sample (0.05–0.5 g) was treated in He flow at *r.t.* (0.5 h) or at 450°C (12 h) before the TPD tests. NH_3 adsorption was performed at *r.t.*, with a 5% NH_3/He mixture. After purging in a He flow for 3 h, thermodesorption was effected by heating to 600 at 10°C min^{-1}. A water trap, consisting of anhydrous KOH, was connected at the outlet of the sample cell in order to avoid water interference on the TCD signal.

Scanning electron microscopy (SEM) was performed on a Philips XL30 apparatus.

Results and discussion

SEM, XRD and TG/DTA analyses of the as prepared compounds

SEM micrographs of $VOPO_4\cdot 2H_2O$ (VOP) and $[Fe(H_2O)]_{0.20}VO_{0.80}PO_4\cdot 2.25H_2O$ (FeVOP) are depicted in Figs 1 and 2, respectively. The VOP samples show a lamellar morphology with some crystals having an evident squared shape (Fig. 1), as expected from structural studies [14, 25]. A similar morphology is shown by FeVOP, suggesting the isomorphous structure of the materials. The crystals of FeVOP, however, appear smaller (Fig. 2), with platelet dimensions of about 1×1 μm *vs.* 25×25 μm of VOP.

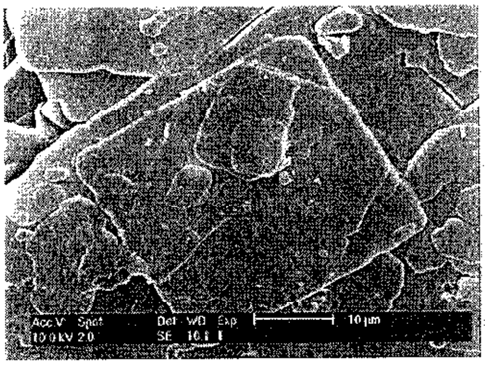

Fig. 1 SEM micrograph of VOP

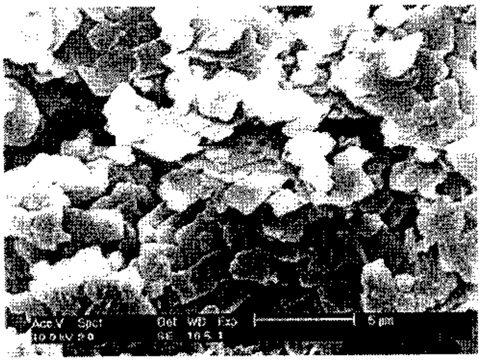

Fig. 2 SEM micrograph of FeVOP

The XRD pattern of FeVOP is shown in Fig. 3, with that of VOP for comparison. FeVOP exhibits a lower degree of crystallinity than VOP. The interlayer distance (d_i) of FeVOP obtained from the first diffraction line at $2\theta=12.45$ is 7.10 Å, a little smaller than that of VOP, which is 7.40 Å. Similarly to VOP, two subsequent (00l) reflections are also evident at 2θ angles 25.02 ($d=3.53$ Å) and 37.87 ($d-2.34$ Å), respectively.

The XRD patterns of FeVOP have also been recorded over the temperature range 20–250°C. Besides the *r.t.* phase, three other phases related, respectively, to the dihydrated, monohydrated and anhydrous compound, are subsequently formed on heating. In Fig. 4 the interlayer spacings of the four differently hydrated phases of FeVOP are shown as a function of the temperature. It can be seen that around 40°C the *r.t.* and dihydrated phases are present together. Dihydrated FeVOP has an interlayer spacing of 6.74 Å. This value is retained up to about 70°C. Then, the interlayer distance slowly decreases. Only in a very small temperature range (72–75°C) are two peaks observed at two different low 2θ angles in the XRD patterns indicating the presence of two phases with d_l=6.62 and 6.41 Å, respectively, the latter corresponding to the monohydrated FeVOP phase. The interlayer distance of this phase also decreases with temperature but, around 110°C it assumes an almost constant value (6.25 Å), maintained up to its disappearance around 150°C. From 140°C the anhydrous phase becomes evident, with an interlayer spacing of 4.21 Å. For the di- and monohydrated phases, the decrease in d_l is also accompanied by a broadening of the diffraction peaks, caused by a slightly disordered stacking of the layers [26]. A similar effect was also observed for the other $[M(H_2O)]_xVO_{1-x}PO_4{\cdot}nH_2O$ compounds [10]. Similarly to VOP [27], after heating at 250°C, anhydrous FeVOP rehydrates when left in air, and gives a XRD pattern similar to that of the as prepared compound. For VOP the dehydration takes place over temperature intervals in which two phases, the di- and monohydrated or the monohydrated and anhydrous phases, are simultaneously present, each one with its own, well defined interlayer distance [10, 28].

The TG/DTA curves of FeVOP are shown in Fig. 5 with those of VOP for comparison. The hydration water is completely lost in three steps in the temperature range 25–230°C, each accompanied by a well resolved endothermic peak. The 0.25 moles of water per mole of compound are lost between 25–40°C. The remaining two moles of water are lost approximately one by one, in two steps in the ranges 50–100 and 100–220°C, respectively. It has been reported [24] that in VOP the two moles of hydration water, lost separately in two steps in the ranges 50–100°C and 100–150°C, are bound to PO_4 and VO groups, respectively. Similarly, it can be supposed that in FeVOP the first lost water is that hydrogen-

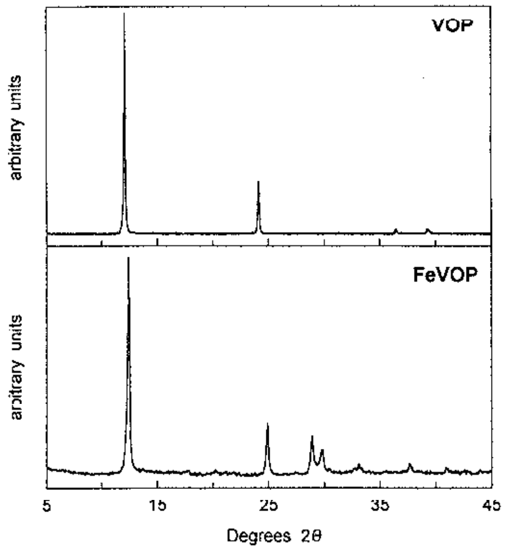

Fig. 3 XRD patterns of FeVOP and VOP

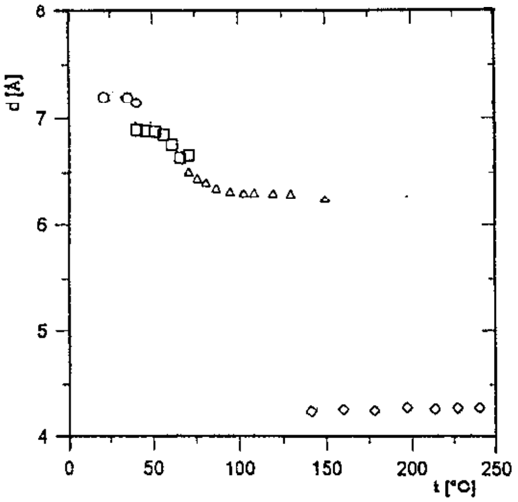

Fig. 4 Interlayer spacings of differently hydrated phases of FeVOP as a function of temperature: (o) *r.t.* phase; (□) dihydrated; (Δ) monohydrated; (◊) anhydrous

bonded to the PO_4 groups, the second is coordinated to VO and $Fe(H_2O)$ groups. The larger, second temperature interval of water elimination for FeVOP could be related to the presence of iron which retains water more strongly than vanadium. The last water coordinated to the iron ions is lost between 300–650°C and above this temperature the material begins to decompose slowly. For anhydrous VOP the decomposition starts later at about 750°C and is accompanied by two sharp endothermic effects.

Ammonia adsorption and NH_3-TPD measurements for the as prepared compounds

The results of NH_3-TPD measurements on VOP samples treated with NH_3 for 4 h (VOP-4) or 24 h (VOP-24) are given in Fig. 6 and Table 1. The spectrum of VOP-4 shows a composite signal with a maximum at 330°C and a shoulder at 250°C. Moreover, a weak intensity signal is present at 120°C. By prolonging the NH_3 adsorption up to 24 h (VOP-24) the intensity of the TPD signal increases, mainly for the component at 250°C which appears as a well defined peak. The total amount of desorbed NH_3 increases with the time of adsorption from 0.74 to $1.05 \cdot 10^{-3}$ mol g^{-1} (Table 1). Such values cannot be explained by surface adsorption: in fact, taking into account the surface area of the VOP sample, 1 $m^2\ g^{-1}$, they would correspond to surface site concentrations of $4–6 \cdot 10^{16}$ cm^{-2}, that is beyond any acceptable surface site concentration; in fact, a surface concentration of VO groups of $2.6 \cdot 10^{14}$ cm^{-2} can be estimated from structural information [13]. This suggests that intercalation of NH_3 occurs between the layers of VOP. As a consequence of NH_3 intercalation, it is expected that the rate of NH_3 adsorption

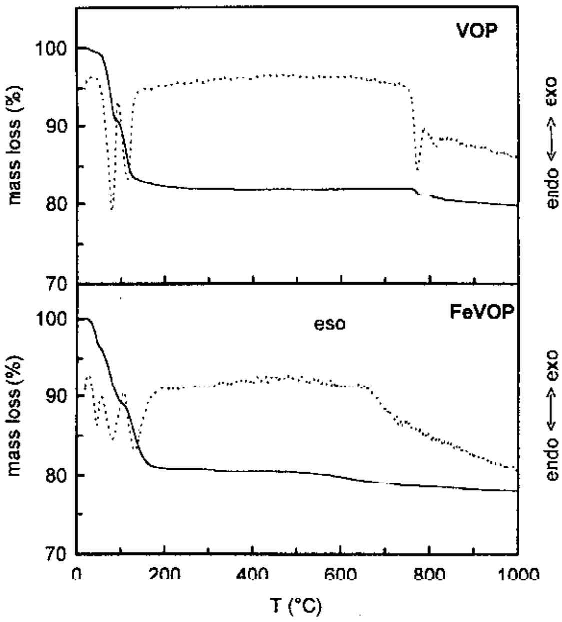

Fig. 5 TG (—) and DTA (···) curves of FeVOP and VOP

can be influenced by diffusive resistances. This could explain the increase in the amount of adsorbed NH_3 with the time of adsorption. Moreover, these resistances could also affect the rate of desorption leading to some delay of the desorption peaks. The shape of TPD spectra, extending over a wide temperature range, suggests the presence of ammonia-adsorbing sites of medium to high strength, the strongest ones prevailing. However, as the TPD signals can be affected by diffusive resistances, the temperatures of the TPD peaks could be higher than those really representing the strengths of NH_3-site interactions. The appearance of two main desorption peaks could be caused by the decrease in the interlayer distance with temperature during the desorption of NH_3, thus hindering the subsequent desorption which needs a higher temperature to occur. However, this effect could also be the consequence of the formation of two different ammoniated phases. This point will be discussed below.

TG/DTA and XRD analyses of the NH_3-treated compounds

TG-DTA curves of VOP-4 and VOP-24 samples are presented in Fig. 7, while the corresponding water losses are given in Table 2. Since the samples release both water and ammonia during heating, the amount of water lost by each compound (moles per mole of compound) is calculated by subtracting from the total loss determined by thermogravimetry the appropriate NH_3 amounts resulting from the TPD spectra (Table 1, last column). Figure 7 shows that in the range 25–500°C, both VOP-4 and VOP-24 undergo a significant mass loss in three

Table 1 Results of the NH_3 TPD measurements

Sample	$T_{Pretreatment}$/°C	$t_{Ads.}$/h	T_{Max}/°C	Desorbed NH_3		
				(mol g^{-1})·10^{5}	(molec cm^{-2})·10^{-14}	(mol mol^{-1})
VOP-4	20	4	330 250(sh)	74	445	0.15
VOP-24	20	24	330 250	105	630	0.21
VOP	450	1	180	0.16	1.8	–
FeVOP-4	20	4	328	148	178	0.30
FeVOP-24	20	24	313	208	250	0.41
FeVOP	450	1	150	2.1	2.4	–

steps, each accompanied by clear endothermic effects. Since the TPD experiments show that up to *ca.* 110°C very little ammonia is desorbed from both materials (Fig. 6), the respective first mass losses, ending around 110°C and associated with a sharp endothermic peak, are only related to the loss of water. The lost amounts (Table 2) are very close to the mole of water lost by pure hydrated VOP

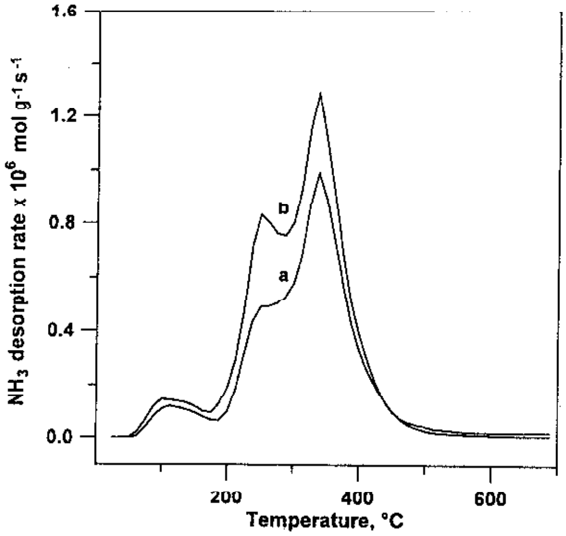

Fig. 6 TPD spectra of VOP treated with NH_3 at *r.t.*: VOP-4 (a) and VOP-24 (b)

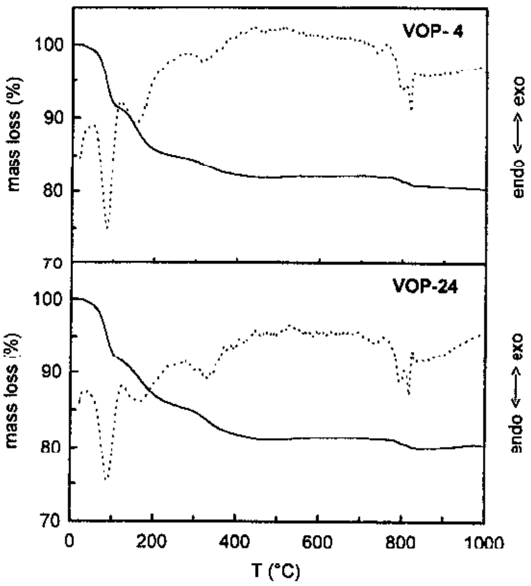

Fig. 7 TG (—) and DTA (···) curves of VOP-4 and VOP-24

Table 2 Amounts of water released by pure and NH_3-treated VOP and FeVOP

Sample	T/ °C	Water loss*/ mol mol^{-1}
VOP	20–100	1.00
	100–170	1.00
VOP-4	20–120	0.94
	120–500	0.93
VOP-24	20–120	0.93
	120–500	0.96
FeVOP	20–100	1.25
	100–200	1.00
FeVOP-4	20–230	1.20
	230–500	0.61
FeVOP-24	20–130	0.60
	130–500	1.40

*For NH_3-treated samples the values are calculated by subtracting the amount of desorbed NH_3 from the total mass losses obtained from TG analyses

in the same temperature range. The subsequent two mass losses occurring in the range 110–500°C, are due to losses of water and ammonia together. This is inferred from the TPD curves, showing two intense NH_3 desorption peaks in this second temperature range. The amounts of water released (Table 2) are very close to the second loss of pure VOP, thus suggesting that the intercalation of

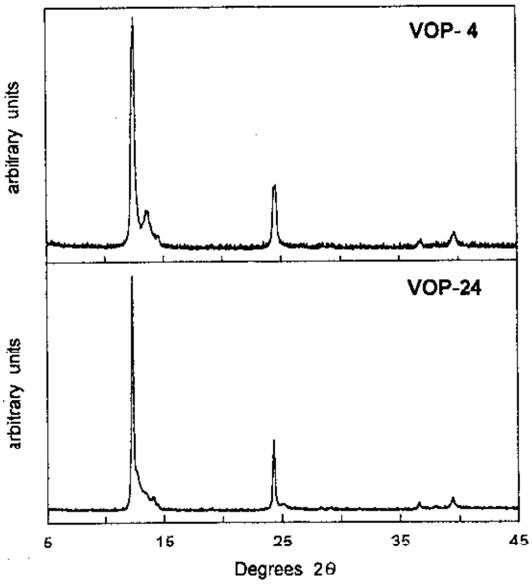

Fig. 8 XRD patterns of VOP-4 and VOP-24

NH_3 does not cause the displacement of water. A very small mass increase, about 0.2%, can be observed in the range 500–750°C, followed by an appreciable mass loss which is accompanied by a composite endothermic effect.

XRD analysis of VOP-4 and VOP-24 (Fig. 8) shows that the compounds retain the layered structure and have a degree of crystallinity slightly lower than that of pure VOP. The interlayer distance is 7.20 Å, a little smaller than that of VOP (7.40 Å). The very weak signals to which the d values 6.56 and 6.10 Å correspond, could be those related the interlayer distances of two other different NH_3-containing phases. Therefore, the appearance of two main desorption peaks in the TPD spectra of VOP-4 and VOP-24 could be explained by the release of ammonia from the two NH_3-VOP phases.

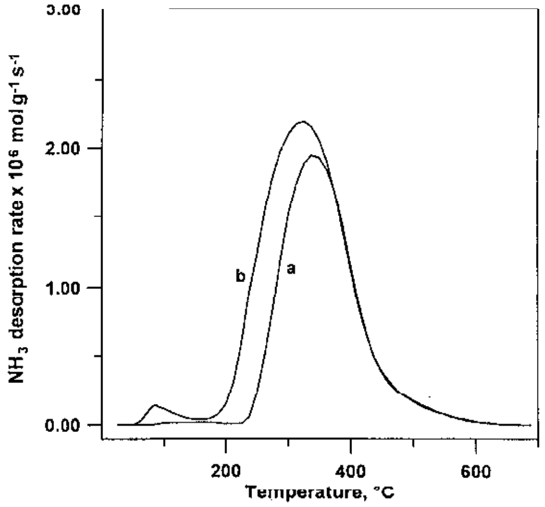

Fig. 9 TPD spectra of FeVOP treated with NH_3 at *r.t.*: FeVOP-4 (a) and FeVOP-24 (b)

The NH_3-TPD spectra of hydrated FeVOP after 4 h (FeVOP-4) and 24 h (FeVOP-24) NH_3 adsorption are reported in Fig. 9. The spectra show tailed peaks with maxima at about 350°C, related to the presence of strong adsorbing sites, with a wide distribution of acid strengths. The increase of adsorption time from 4 to 24 h leads to an increase in peak intensity. At the same time, the temperatures of the start of desorption and peak maxima decrease. The first effect suggests that the adsorption rate is limited by diffusion in the interlayer space, as discussed for VOP. The latter effect could be explained by the presence of adsorption sites with different strengths, the increase of adsorption time leading to a progressive coverage of the weaker ones. The amounts of desorbed NH_3 from FeVOP-4 and FeVOP-24 (Table 1) correspond to surface concentrations of $1.8\ 2.4\ 10^{16}$ molecule·cm^{-2}. These values are much higher than admissible for a surface site concentration, suggesting that NH_3 adsorption also occurs in the interlayer space of FeVOP.

It is worth noting that, disregarding the small peak at low temperatures, NH_3 is desorbed from FeVOP samples in a single step, differently from VOP. This could be related to the higher crystalline disorder of FeVOP in comparison with the VOP sample. The narrowing of the interlayer distance with temperature, probably occurs more gradually, allowing a continuous release of the adsorbed ammonia.

The TG/DTA curves of FeVOP-4 and FeVOP-24 samples are shown in Fig. 10. The mass loss occurs in two steps for both materials. Taking into account the TPD curves (Fig. 9) and the data in Table 1, the first mass losses, ending at about 130°C for FeVOP-4 and 230°C for FeVOP-24, must be ascribed to water only, while the second ones, ending around 500°C, refer to the simultaneous release of water and ammonia. The amounts of released water are listed in Table 2. The values are very close to those of NH_3-free samples, thus suggesting that NH_3 intercalation in hydrated FeVOP occurs without displacement of hydration water, as also observed for hydrated VOP. The TG curves show a small (1–1.1%) increase in weight in the temperature range 500–800°C, as observed for VOP, but to a lower extent. This could be explained by supposing that the materials undergo some reduction during NH_3 treatment and afterwards are reoxidized during heating in an air flow. The very small extent of weight gain suggests that this phenomenon only involves the surface of the solids. It is worth noting that the weight increases for FeVOP and VOP are roughly in the same ratio as their specific surface areas.

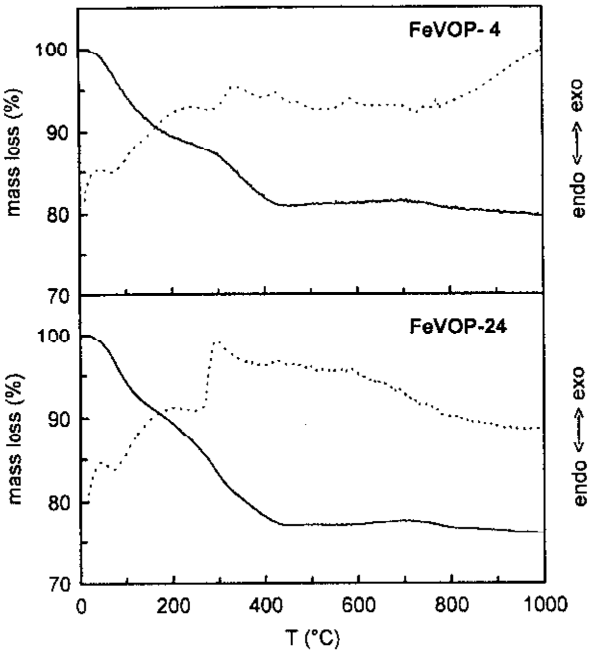

Fig. 10 TG (—) and DTA (···) curves of FeVOP-4 and FeVOP-24

XRD patterns of FeVOP-4 and FeVOP-24, reported in Fig. 11, show that the layered structure is retained. The pattern of FeVOP-4 accounts for a material with a degree of crystallinity of the same order as that of the starting FeVOP. The solid is a pure phase with an interlayer distance of 6.52 Å, reduced with respect to that of FeVOP. FeVOP-24, on the contrary, is a less crystalline material than FeVOP-4 or FeVOP. Two phases are present in the solid, with interlayer spacings of 6.86 and 6.52 Å, the phase with the lower d_i value being in a higher amount. This latter should correspond to the FeVOP-4 phase. The TPD spectrum of FeVOP-24 does not allow to distinguish between the two different ammoniated phases, unlike VOP samples. It can be supposed that FeVOP exhibits a wider heterogeneity of the acid sites, leading to broader TPD peaks. This effect could prevent the resolution of the signals which should come from the different ammoniated phases.

The above results have shown that hydrated VOP and FeVOP adsorb significant amounts of ammonia. The process does not destroy the layered structure and always gives rise to materials with interlayer spacings smaller than those of the parent compounds. Ammonia intercalation occurring in hydrated VOP and FeVOP samples without displacement of water and with reduction of the interlayer spacing, suggests the presence of strong interactions between the layers promoted by the presence of NH_3. Different mechanisms of interaction between NH_3 and adsorbing sites can be hypothesized. It is our opinion that NH_3 is protonated by H_2O, whose acidic strength is enhanced by coordination to the Fe and V=O groups according to the following scheme (1) (L stands for Fe or V=O):

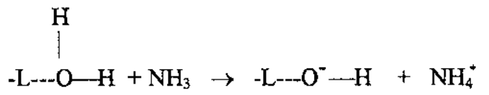

$$-\mathrm{L}{-}{-}{-}\overset{\overset{\mathrm{H}}{|}}{\mathrm{O}}{-}\mathrm{H} + \mathrm{NH_3} \rightarrow -\mathrm{L}{-}{-}{-}\mathrm{O}^{-}{-}\mathrm{H} + \mathrm{NH_4^+}$$

(1)

This mechanism could explain the decrease in interlayer distance as a consequence of strong ionic interactions between negatively charged layers and NH_4^+ ions. A contraction of interlayer spacing was reported for intercalation of cations such as Co^{2+}, Ni^{2+}, Fe^{3+} [29], alkali and alkaline earth metals [30, 31], or benzidine [19] into VOP and it was found that the hydration water was more tightly retained in the intercalation compounds than in pure VOP. Moreover, in some cases, the process of intercalation gave rise to the formation of different phases due to alternate filling of interlayer spaces [30]. It can be supposed that a similar process also occurs in the presence of ammonium ions. This would agree with XRD data (Fig. 6), which give indication of the presence of different ammoniated phases.

NH_3 adsorption and NH_3-TPD measurements for the anhydrous materials

Different TPD spectra are obtained when NH_3 adsorption is performed on VOP and FeVOP treated at 450°C (Fig. 12). Broad and tailed signals are observed, with maxima at about 180 and 150°C for VOP and FeVOP, respectively. These can be related to the presence of acid sites with a wide range of acid strengths, the weaker ones prevailing. In comparison with the hydrated materials, the amounts of desorbed NH_3 are two orders of magnitude smaller, suggesting that adsorption occurs only on the external surface of crystallites. Surface concentrations of adsorbing sites can be evaluated by taking into account the crystalline structure. As shown by SEM micrographs (Figs 1 and 2), the materials consist of platelet shaped crystals that preferentially expose faces corresponding to planes of the layered structure. The density of VO groups on such planes, calculated from structural data [13], is $2.6\cdot10^{14}$ cm^{-2} in VOP, while in FeVOP 20% of the VO groups, that is $0.5\cdot10^{14}$ cm^{-2}, are replaced by Fe atoms. Half of the VO groups (because V=O bonds point alternately inside and outside the crystal) and all Fe atoms have a free coodination site. Thus the theoretical surface concentration of coordination sites is of $1.3\cdot10^{14}$ cm^{-2} for VOP and $1.5\cdot10^{14}$ cm^{-2} for FeVOP. Since these values are of the same order of magnitude as the concentration of the NH_3 molecules (Table 1), it can be supposed that NH_3 adsorption only occurs on the external surface of the heat-treated materials. This is confirmed by the observation that the materials treated at 450°C are saturated with NH_3 within a few minutes (less than 30 min), suggesting that diffusive effects are negligible, as expected for a surface adsorption. Of course, diffusive limitations should be absent also during desorption, so the temperatures of TPD signals could really be representative of the strength of interaction of NH_3 and acid sites. This could explain why the temperatures of the desorption peaks are lower than those observed for hydrated materials. The wide distribution of acid strength suggests the presence of a great surface heterogeneity.

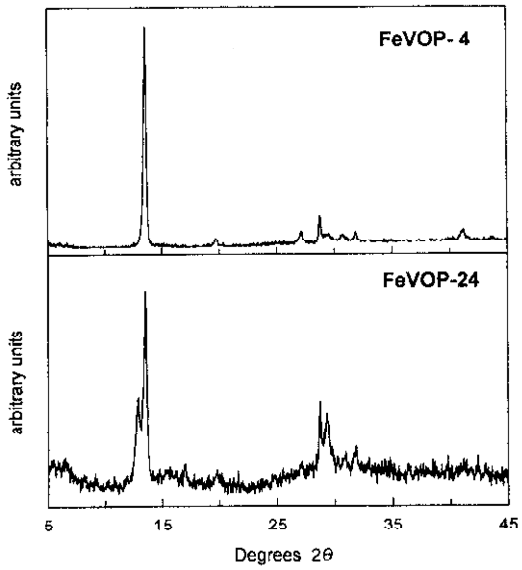

Fig. 11 XRD patterns of FeVOP-4 and FeVOP-24

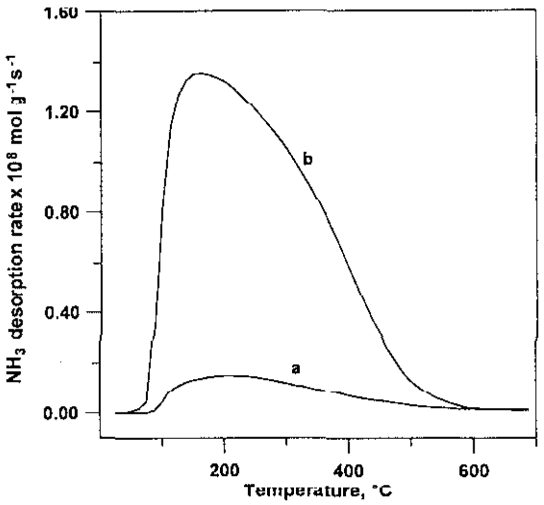

Fig. 12 TPD spectra of FeVOP (a) and VOP (b) after treatment in a He flow at 450°C and saturation with NH_3 at *r.t.*

The above results show that the intercalation of NH_3 between the layers occurs with hydrated VOP and FeVOP, but not with anhydrous materials. A similar behaviour was observed for layered phosphates of zirconium and other tetravalent metals [21, 22], where the heat treatment led to elimination of water and formation of chemical bonds between layers, which hindered the intercalation of ammonia. However, it seems unlikely that the formation of chemical bonds between layers can occur in vanadyl phosphate, given the absence of condensing groups. It can be supposed that the decrease in interlayer distance as a consequence of dehydration, strongly hinders the NH_3 access in the interlayer region. However, it cannot be excluded that the presence of water is need to promote the intercalation of NH_3. This effect could be explained by the hypothesis of protonation of ammonia by hydration water, as discussed above.

Conclusions

A new material, with a good degree of crystallinity isomorphous with pure $VOPO_4 \cdot 2H_2O$ has been prepared by partial substitution for VO groups by Fe atoms. Heat treatment at temperatures up to 650°C does not destroy the layered structure. In the hydrated materials NH_3 is intercalated with strong interactions and without water displacement. On the other hand, with heat-treated materials the adsorption of NH_3 only occurs on the external surface of the crystallites and allows to characterize surface acidity. A wide distribution of acid strengths is observed. The Fe^{3+}-containing material possesses a higher surface concentration of acid sites in comparison with pure vanadyl phosphate but exhibits a similar acid strength distribution. The nature of interaction of NH_3 with acid sites deserves further investigation.

* * *

The authors thank Mrs. Clelia Zucchini and Mr. Sabatino Russo of Istituto di Ricerche sulla Combustione, CNR, Naples (Italy) for performing SEM measurements. Funds from MURST are also acknowledged.

References

1 G. J. Hutching and R. Higgins, J. Catal., 162 (1996) 153.
2 G. Centi, Catal. Today, 16 (1993) 5.
3 G. Centi, F. Trifirò, J. R. Ebner and M. V. Franchetti, Chem. Rev., 88 (1988) 55.
4 B. K. Hodnett, Catal. Rev. Sci. Eng., 27 (1985) 373.
5 Y. Takita, S. Kikukawa, Y. Abe, Y. Mizukawa and T. Shihara, Nippon Kagaku Kaishi, (1992) 354.
6 A. Martin, B. Lücke, H. Seeboth and G. Ladwig, App. Catal, 49 (1989) 205.
7 A. Martin, B. Lücke, H. Seeboth, G. Ladwig and E. Fischer, React. Kinet. Catal. Lett., 38 (1989) 33.
8 K. Melanová, J. Votinsky, L. Beneš and V. Zima, Mat. Res. Bull., 30 (1995) 1115.
9 K. Richtrová, J. Votinsky, J. Kalousová, L. Beneš and V. Zima, J. Solid State Chem., 116 (1995) 400.
10 L. Beneš, P. Galli, M. A. Massucci, K. Melánová, P. Patrono and V. Zima, J. Thermal Anal., 50 (1997) 355.
11 V. A. Zazhigalov, J. Haber, J. Stoch, I. V. Bacherikova, G. H. Komashko and A. I. Pyatnitskaya, App. Catal. A: General, 134 (1996) 225.
12 M. T. Sananés-Schulz, F. Benabdelouahab, G. I. Hutchings and J. C. Volta, J. Catal., 163 (1996) 346.
13 L. Beneš, J. Votinsky, J. Kalousová and J. Klikorka, Inorg. Chim. Acta, 114 (1986) 47.
14 H. R. Tietze, Austral. J. Chem., 34 (1981) 2035.
15 M. Tachez, F. Theobald, J. Bernard and A. W. Hewat, Rev. Chim. Min., 19 (1982) 292.
16 J. Votinsky, L. Beneš, J. Kalousová and J. Klikorka, Inorg. Chim. Acta, 126 (1987) 19.
17 L. Beneš, R. Hyklová, J. Kalousová and L. Votinsky, Inorg. Chim. Acta, 177 (1995) 71.
18 A. De Stefanis and A. A. G. Tomlinson, J. Mater. Chem., 5 (1994) 319.
19 A. De Stefanis, S. Foglia and A. A. G. Tomlinson, J. Mater. Chem., 5 (1995) 375.
20 F. Benabdelouahab, J. C. Volta and R. Olier, J. Catal., 148 (1994) 334.
21 M. Turco, P. Ciambelli, G. Bagnasco, A. La Ginestra, P. Galli and C. Ferragina, J. Catal., 117 (1989) 335.
22 G. Bagnasco, P. Ciambelli, A. La Ginestra and M. Turco, Thermochim. Acta, 162 (1990) 91.
23 G. Bagnasco, P. Ciambelli, A. Frezza, P. Galli, A. La Ginestra and M. Turco, App. Catal., 68 (1991) 381.
24 G. Ladwig, Z. Anorg. Allg. Chem., 338 (1965) 266.
25 L. Beneš and V. Zima, J. Incl. Phenom. Molec. Recog. in Chem., 20 (1995) 381.
26 S. Hendricks and E. Teller, J. Phys. Chem., 10 (1942) 147.
27 E. Bordes, Catal Today, 1 (1987) 499.
28 V. Zima, L. Beneš, J. Málek and M. Vlček, Mat. Res. Bull., 29 (1994) 687.
29 M. R. Antonio, R. L. Barbour and P. R. Blumm, Inorg. Chem., 26 (1993) 1235.
30 R. Šišková, L. Beneš, V. Zima, M. Vlček, J. Votinsky and J. Kalousová, Polyhedron, 12 (1993) 181.
31 J. W. Johnson and A. J. Jacobson, Angew. Chem. Int. Ed. Engl., 22 (1983) 412.